ATLAS NOTE

March 10, 2013

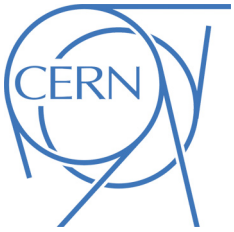

Layman study of non-resistive and resistive micromega detectors proposed for the ATLAS upgrade

J. Connors[a], L. Jeanty[a], M. Franklin[a], P. Giromini[a,b]

[a]*Harvard University, Cambridge, Massachusetts 02138*
[b]*Laboratori Nazionali di Frascati, Istituto Nazionale di Fisica Nucleare, Frascati, Italy*

Abstract

We have studied the performance of 10x10 cm^2 micromega prototypes with a conductive-anode readout or with a resistive anode built on top of readout electrodes. Resisitive micromegas were developed to mitigate the effects of sparks, either spontaneous or induced by highly ionizing particles. Sparks discharge the cathode-anode capacitance of the entire non-resistive detector, disable it for a fraction of a second and may potentially destroy the mesh or the the readout electronics. In a resistive micromega, sparks bring locally the resistive anode to the mesh potential and the energy involved is quite small. We have indeed operated our resistive micromega with rates of spontaneous sparks as large as 60 kHz without any damage. However, this notable improvement comes with a price tag. First, the readout electrodes of the resistive micromega collect one half of the charge, produced by ionizing particles, that is collected by the conductive-anode readout. Amplification gains $\simeq 10^4$ are reached for voltages quite close to the breakdown point. The salient feature of the micromega technique - fast evacuation of the positive ions ($\leq$ 200 ns) from the amplification gap- is watered down because the readout-electrode current is additionally induced for several microseconds by the diffusion of the ionization charge accumulated on the resistive strips. Lastly, the I-V curve of the resistive micromega becomes similar to that of a Zener diode, the dynamic impedance being provided by spontaneous-spark shedding at the breakdown voltage. The tolerance of this knee voltage over a larger-size detector will be crucial because the spot with the lowest avalanche voltage will fix the operating voltage and maximum gain of the entire detector.

1 Micromega detectors

The amplifying gaps of our resistive and non-resistive micromegas are 128 μm thick. The cathode is a woven stainless mesh with 400 lines/in and a wire thickness of 18 μm. The mesh is kept at the 128 μm distance from the anode by a matrix of Pyralux pillars with 400 μm diameter and spaced by 2 (2.5) mm for the non-resistive (resistive) chamber in the x and y direction.

The anode of the non-resistive chamber is a 1 mm FR4 board cladded with a layer of 18 μm copper foil. The copper is etched into readout strips 0.9 mm wide, 10 cm long, with a 1 mm pitch. The gap between copper strips is not filled with insulator. The cathode-anode capacitance is about 1.5 nF.

The anode of the resistive chamber (see Fig. 1) consists of resistive strips 64 μm thick, 100 mm long in the x direction, 180 μm wide, and with a 250 μm pitch. Each resistive strips is connected to ground with a 45 MΩ resistor. The resistance of each strip is 5 MΩ/cm. The 70 μm gaps between resistive strips are filled with insulator. The resistive layer is built on top of the y-readout electrode. The y electrode consists of 18 μm thick copper strips, 80 μm wide, with a 250 μm pitch and 10 cm long in the y direction. The y readout is separated from the resistive anode by a 64 μm layer of photo-imageable cover-lay. A similar cover-lay separates the y readout from the x readout which consists of 18 μm thick copper strips, 200 μm wide, with a 250 μm pitch, and 10 cm long in the x direction. The y readout is built on top of a 1 mm thick FR4 board, copper cladded and grounded on the opposite side. The capacitance of the mesh with respect to the resistive-anode plane is measured to be about 1.7 nF, that between the resistive anode and the y-readout plane is about 6-7 nF, and that between the y- and x-readout planes about 15 nF. The capacitance between the x-readout plane and ground is about 2.8 nF. The drift gap is built on top of the

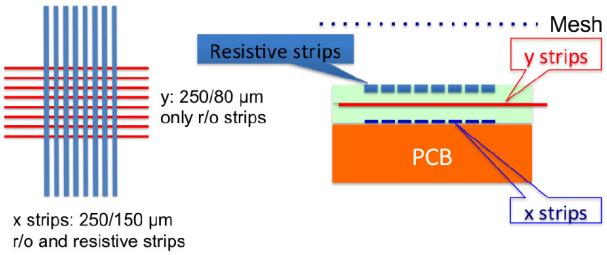

Figure 1: Resistive chamber sketch. Readout trip layout (left): the bottom x-readout strips are parallel to the resistive strips and orthogonal to the y-readout strips. Vertcal cross section (right). The figure is reproduced from Ref. [1].

amplifying gap. Its thickness is 5 mm for the resistive chamber and 25 mm for the non-resistive one.

2 Electronics

The micromega high voltage is supplied by a CAEN N1470 unit which also measures the current drawn by the chamber to a 10 nA accuracy with a 5 Hz frequency. The mesh is set to negative voltages between 400 and 1000 V depending on the gas mixture. The electric field across the drift gap is set to (100 – 200) V/cm, also depending on the gas mixture.

We measure the micromega amplification factor or gain by using Fe^{55} sources (15 nCi and 10 μCi) and assuming that 6 keV photons produce 300 electron-ion pairs in the drift volume. The charge of the signal induced on the mesh or on the sum of all readout strips is integrated with an ORTEC 142C preamplifier. Since its charge integrating capacitor is fed back to its input, this amplifier drains all charge produced in the amplifying gap. When performing spark studies, in which there are significant voltage swings at the preamp input, we decouple it with a 9.4 nF capacitor. We also use a CANBERRA 1406

Table 1: Measured breakdown voltages of non-resistive micromegas are compared to the Paschen expectation for several gas mixtures.

Gas	Observed	Expected
Air	950 V	1430 V
N_2	800 V	975 V
CO_2	1000 V	1995 V
Argon	350 V	430 V

preamplifier which has in input a 2 nF decoupling capacitor. When using decoupling capacitors, we correct the measured gain for the charge-drain deficit $c_{in}/(c_{in} + c_D)$, where c_{in} and c_D are the decoupling and detector capacitances, respectively. The 142C has a few ns rise-time and a 1 ms fall-time; the 1406 has a 100 ns rise-time and 70 μs fall-time. The preamp output is fed to an ORTEC 472A shaping amplifier (1 μs shaping time), the output of which is recorded with a kicksorter. The gain of the electronic chain is monitored by injecting a known amount of charge into the preamp test input.

We also measure the current induced by particle ionization and sparks on the mesh and readout electrodes using a Lecroy 612AM amplifier, with a gain of 50, fed through a 50 Ω cable.

3 Micromega conditioning

Both resistive and non-resistive micromega were built at the CERN PCB facility. So far, we have tested two non-resistive and one resistive amplifying gap. Upon arrival, we apply voltage to the chambers filled with air. We monitor the chamber current and the rate of sparks with a 10 MΩ probe connected to the mesh through a 10 nF HV capacitor. At the beginning, all chambers draw significant current and spark at about 600 V. We limit the dark current to a few microamps and increase the mesh voltage every once in a while in order to burn out the dust/dirt in the amplifying gap. In a few hours, the non-resistive chambers are cleaned and can hold almost 1 kV without any dark current or sparks. The same procedure works for the resistive chamber which can hold 1 kV without discharges after several days of toasting rather than a few hours of burning.

4 Micromega gain and breakdown voltages

For a given gas mixture, the attainable gain is limited by the breakdown voltage. Breakdown voltage is defined at first as the voltage at which one detects voltage spikes on the mesh, protected by a 20 MΩ resistor, with a frequency of about 0.1 Hz [1]. These breakdown voltages for both resistive and non-resistive chambers are lower than what is expected from the Paschen's curves [3] at atmospheric pressure and for a gas thickness of 128 μm (see Table 1 for the non-resistive micromega).

When irradiating the non-resistive micromega with a 1 mCi ^{207}Bi source, the breakdown voltages decrease significantly. This does not happen in the resistive micromega in which the anode does not have sharp edges because the gaps between resistive strips are filled with insulator.

We have measured the micromega gain for several gas mixtures with a ^{55}Fe source illuminating most of the chamber area. The charge produced by the 6 keV photon is integrated with the 142C preamp, directly connected to the mesh. The mesh, in turn, is connected to the HV power supply with a 10 MΩ

[1] The micromega I-V curve at the breakdown voltage is discussed in the last section.

resistor, followed by a low-pass filter with a 100 ms RC constant that cuts the 50 Hz noise of the HV power supply (see Fig. 2).

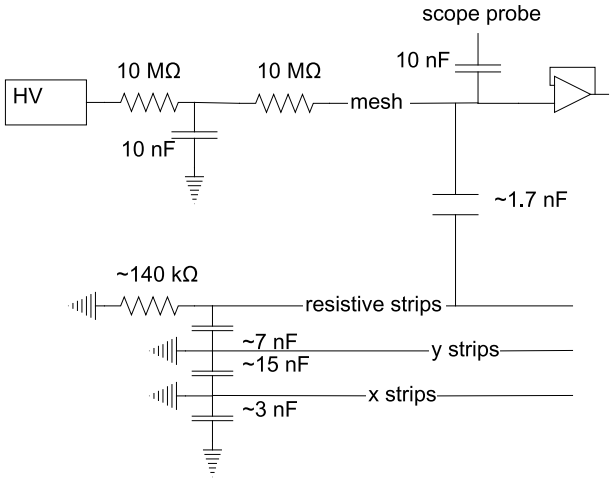

Figure 2: Sketch of the electric circuit used to detect signals on the mesh for the resistive micromegas chamber.

Fig. 3 shows the charge distribution of the 6 keV line and of the argon-escape peak when using the non-resistive micromega with a 97% argon and 3% ethane mixture. The resolution of the 6 keV line is about 14%.

Fig. 4 shows the same distribution for the resistive micromega fed and read as the non-resistive one. In this case, the y strips are grounded as well as the resistive strips. The increase of the noise level is an artifact due to the thicker entrance window of the resistive chamber.

The charge induced on the mesh of the resistive chamber is 72% of that of the non-resistive one. This reduction can be calculated using Ramo's theorem [4]. In the non-resistive micromega, the current induced by the moving ionization between the amplifier on the mesh and the anode is $i = qvE_w$, where q is the ionization charge, v its velocity, and E_w is the weighting field which for the non-resistive micromega is $1/d$, d being the thickness of the amplifying gap. In the resistive micromega, under the assumption that resistive strips are isolated during the ionization collection (≤ 200 ns), the induced current flows between the preamp on the mesh and the y strips at ground. In this case, $E_w = 1/(d(1 + 1/\epsilon)) = 0.72/d$, where $\epsilon = 2.6$ is an educated guess of the average dielectric constant of the Pyralux and the resistive material separating the amplifying gap from the y strips. The measured ratio of the average response of the two detectors is reproduced by calculating with static weighting fields the current induced by the moving ionization only. However, the calculation neglects the signal induced by the time-dependent reaction of the resistive strips. The latter contribution likely explains the broadening of the 6 keV line in the resistive chamber (the resolution degrades from 14 to 22%, relative to that of the non-resistive chamber).

Table 2 lists the maximum gains attainable with the non-resistive micromegas for different gas mixtures. We also list breakdown voltages in absence of ionizing radiation (BVNR) and with a rate of several kHz/cm^2 induced by the ^{207}Bi source (BVR). We note that Ar+C_2H_6 is the only mixture that provides gains larger than 10^4 before sparks occur. We also observe that the difference between the breakdown voltages BVNR and BVR depends on the gas mixture, and is small for the 97% Ar+3% C_2H_6 mixture. For these reasons, we first used this mixture to test the resistive micromega. With this gas mixture, the BVNR and BVR values in the resistive chamber are the same, and equal to the BVNR of the non-resistive chamber.

However, when using Ar+CO_2 mixtures, the breakdown voltages in the resistive chamber are much

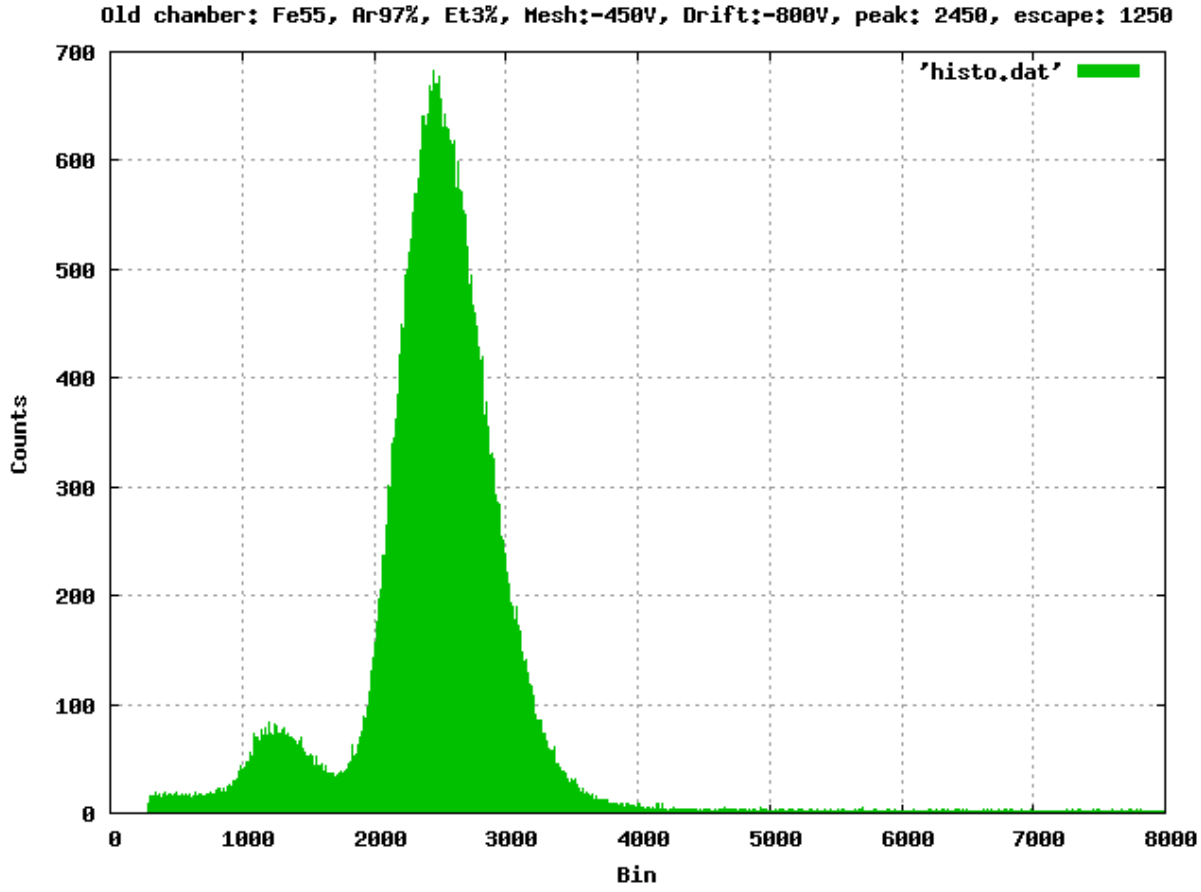

Figure 3: Charge distribution (arbitrary units) of the signals induced by a a ^{55}Fe source on the mesh of the non-resistive micromega filled with a 97%Ar+3%C_2H_6 mixture.

higher than in the non-resistive detector. When using a 97% Ar+3%CO_2 mixture, BVNR≃BVR≃ 570 V and, at 560 V, the micromega gain at the mesh is 16,700. Fig. 5 shows the resistive-micromega gain as a function of the voltage.

We also measure the charge of the 6 keV signal induced on the *y* electrodes. As shown in Fig. 6, we stabilize the mesh voltage with a 100 nF capacitor.

For a non-resistive chamber, the gains measured at the mesh and at the anodic electrode are the same. For the resistive micromega operated at 560 V, the gain at the *y* readout is 11,000, a 34% reduction of the signal at the mesh (16,700). As shown in the next section, the current signals induced on the *y* electrode have a slow component that lasts microseconds, and the charge integrated from the readout electrodes appears smaller because of the ballistic deficit in the shaping amplifier. Since the mesh signal decreases by 38% relative to the mesh signal on the non-resistive chamber because of the reduced weighting field, the gain of the resistive micromega at the *y* electrode is a factor of two smaller than that of a non-resistive micromega, consistent with what measured in [2]. All things included, the resistive micromega can provide gains of the order of 10^4 with an Ar+CO_2 mixture with a mesh voltage of 560 V and no sparks. At 570 V (gain of 17,000 at the *y* electrode) we measure a spontaneous-spark rate of several Hz.

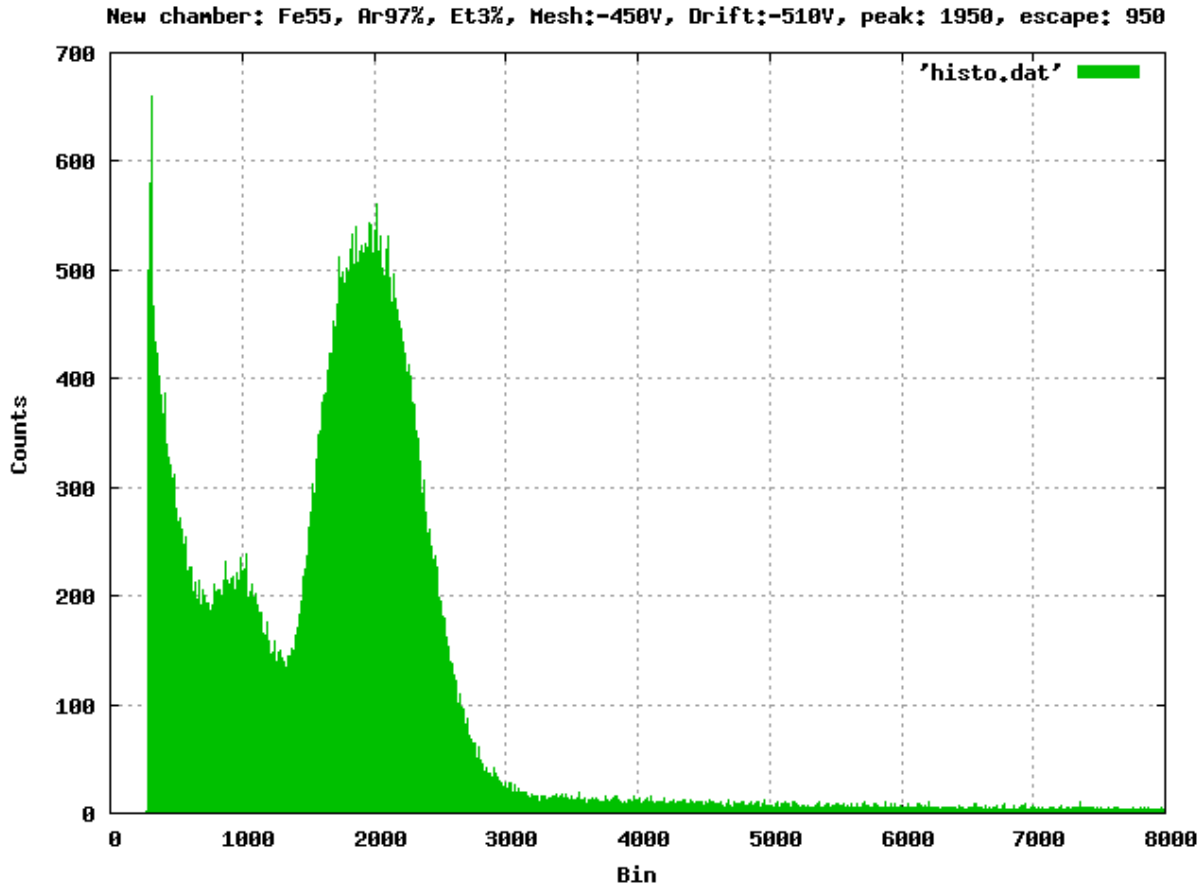

Figure 4: Charge distribution (arbitrary units) of the signals induced by a a Fe^{55} source on the mesh of the resistive micromega filled with a 97%Ar+3%C_2H_6 mixture.

Table 2: Maximum gain of non-resistive chambers for different gas mixtures. The breakdown voltages without irradiation (BVNR) and for a radiation rate of several kHz/cm^2 (BVR) are also listed.

Gas Mixture	Max Gain at mesh V	BVNR	BVR
CO_2	1200 at 960 V	1000 V	960 V
90% Ar + 10% CO_2	2500 at 510 V	540 V	480 V
81% Ar + 19% CO_2	4000 at 520 V	600 V	510 V
90% Ar + 10% CH4	5000 at 550 V	580 V	550 V
90% Ar + 10% C_2H_6	26000 at 500 V	550 V	520 V
95% Ar + 5% C_2H_6	26000 at 460 V	490 V	470 V
97% Ar + 3% C_2H_6	30000 at 450 V	470 V	460 V
85% Ar + 15% C_2H_6	32000 at 550 V	580 V	570 V

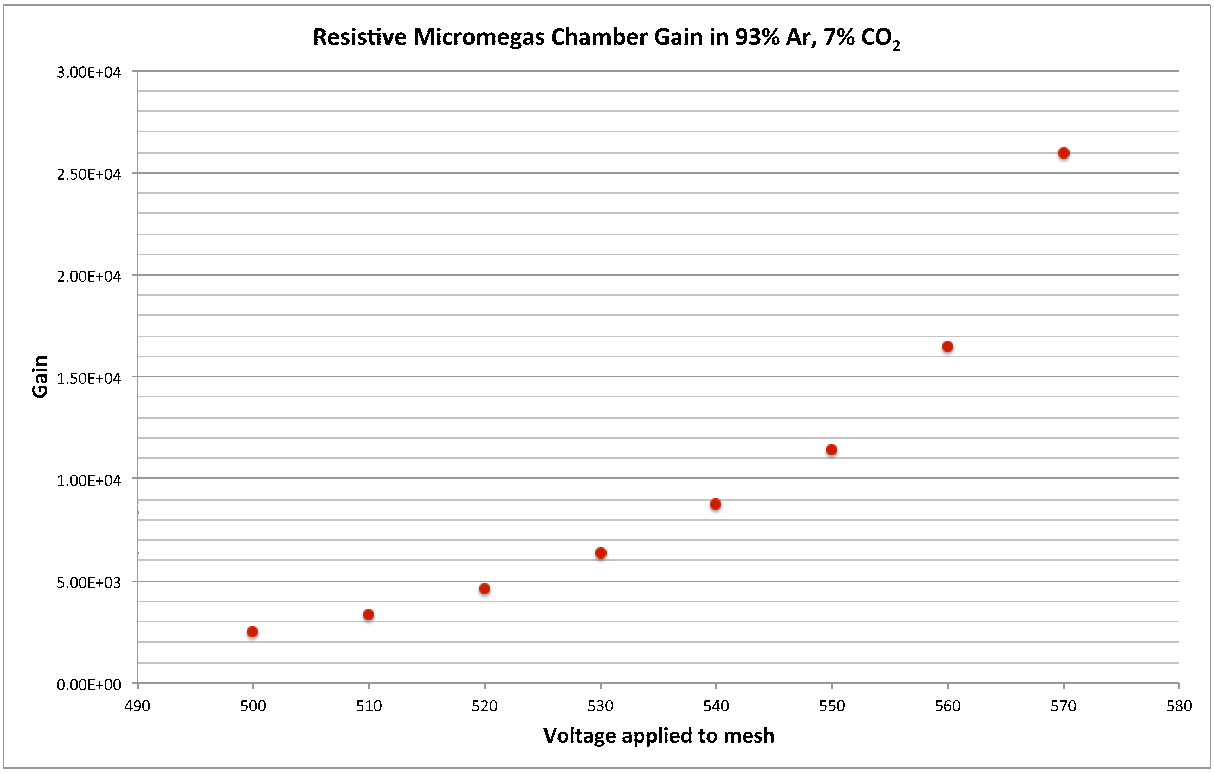

Figure 5: Gain of a resistive micromega filled with a 97% Ar + 3% CO_2 mixture as a function of the mesh voltage. The signal is read from the mesh.

5 Signal shapes as a function of time

Figure 7 shows the response of the 1406 preamp, connected to the mesh, to a 6 keV photon for the non-resistive and resistive micromegas, respectively. The y electrode of the resistive chamber is grounded. We use a 97% Ar+3% C_2H_6 mixture and a mesh voltage of -450 V.

For the non-resistive micromega, the induced charge is integrated in a fraction of a microsecond, and then the charge-amplifier output falls exponentially in about 70 μs. In the case of resistive chamber, the signal peak is followed by a wiggle that lasts microseconds. The maximum pulse height corresponds to the end of the ionization collection during which time the resistive strips are mostly isolated. The wiggle is induced by the ionization charge accumulated on the resistive strips that diffuses along them. Using the Telegraph equation, one expects the diffusion time constant to be of the order of 5 MΩ/cm $\times$ 2 pf/cm = 10 μs (the capacitance between the 328 resistive strips and the mesh is 1.7 nF and that between the resistive and y strips is about 6 nF).

Figs 8 shows the simultaneous response of the 1406 connected to the mesh and the 142C connected to the x strips, with the y strips floating. Following the peak of the ionization collection, the x-readout preamp continues to integrate the current induced by the charge diffusing along the parallel resistive strips.

Figs 9 shows the simultaneous response of the 1406 connected to the mesh and the 142C connected to the y strips, with x strips floating. Because the y strips are perpendicular to the dispersion path, they light up in sequence and the integrated charge peaks after several microseconds. It will be our interest to study how charge dispersion affects the resolution of the VMM1 front-end electronics that provide the charge integrated peak amplitude and time with respect to the bunch-crossing clock.

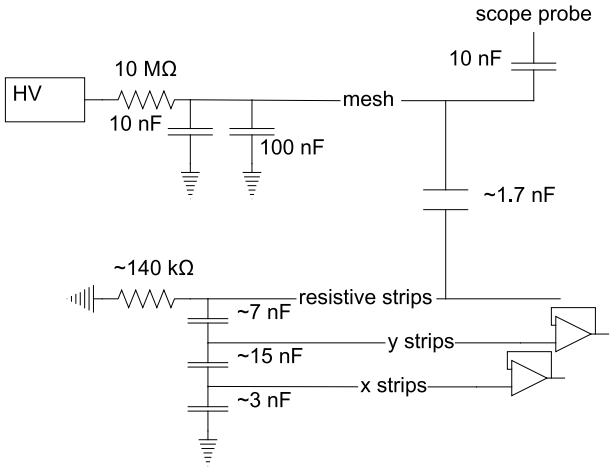

Figure 6: Sketch of the electric circuit used to detect signals on the readout electrodes for the resistive micromegas chamber.

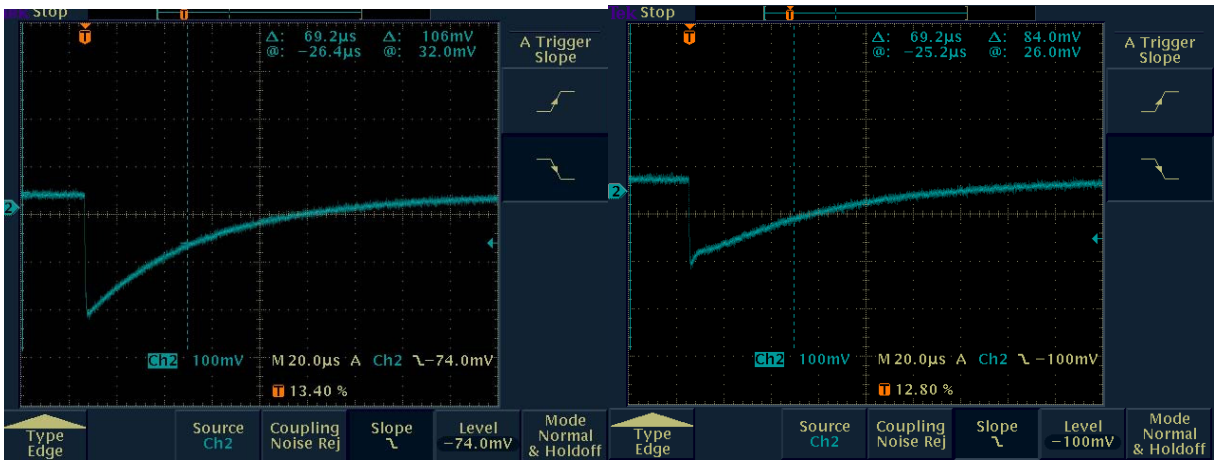

Figure 7: Typical 1406 pulse induced by a 6 keV photon in the (left) non-resistive and (right) resistive micromegas.

One appealing feature of the original non-resistive micromega is that no current flows in the detector after the $\leq$ 200 ns needed to collect all ions produced in the signal amplification. In the resistive micromega, current continues to flow in the detector for several microseconds after the passage of a particle.

6 Spark studies

We use a 97%A+3%C_2H_6 mixture for the initial spark studies. We set the mesh voltage at -470 V as in Fig. 2. For the resistive micromega, we also ground the *y* strips. We look at sparks on the mesh with the 1406 preamp and with a probe decoupled with a 10 nF capacitor. We irradiate the chambers with a 15 nCi ^{55}Fe source or send pulses to the preamp test input to monitor its response following a spark. Figure 10 shows a typical spark signal together with ^{55}Fe signals for the non-resistive micromega. Typical spark signals accompanied by test pulses are shown in Fig. 11 for the resistive micromega.

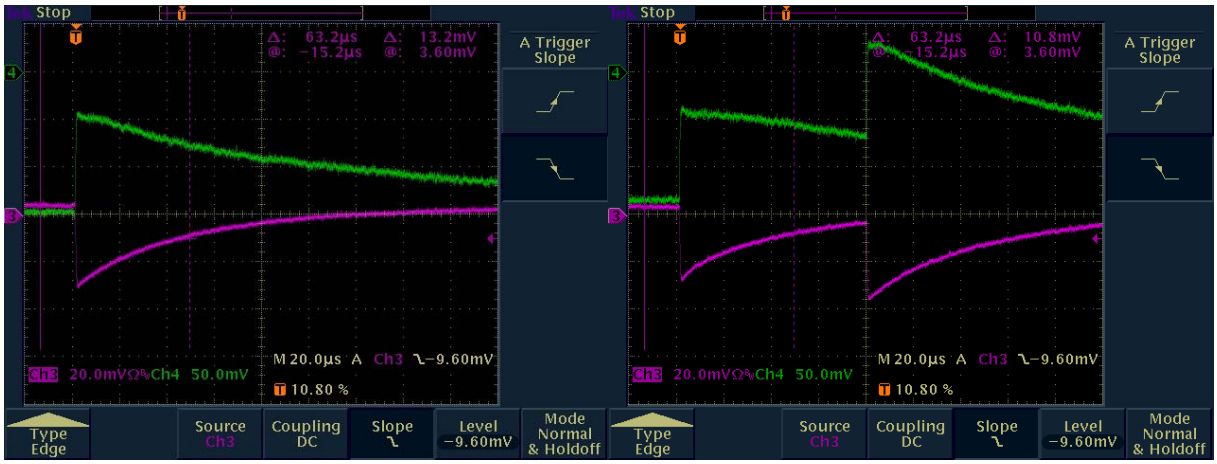

Figure 8: Typical pulses induced by a 6 keV photon on the mesh (ch. 3, magenta) and on the x strips (ch. 4, green) of the resistive micromega. The y strips are floating.

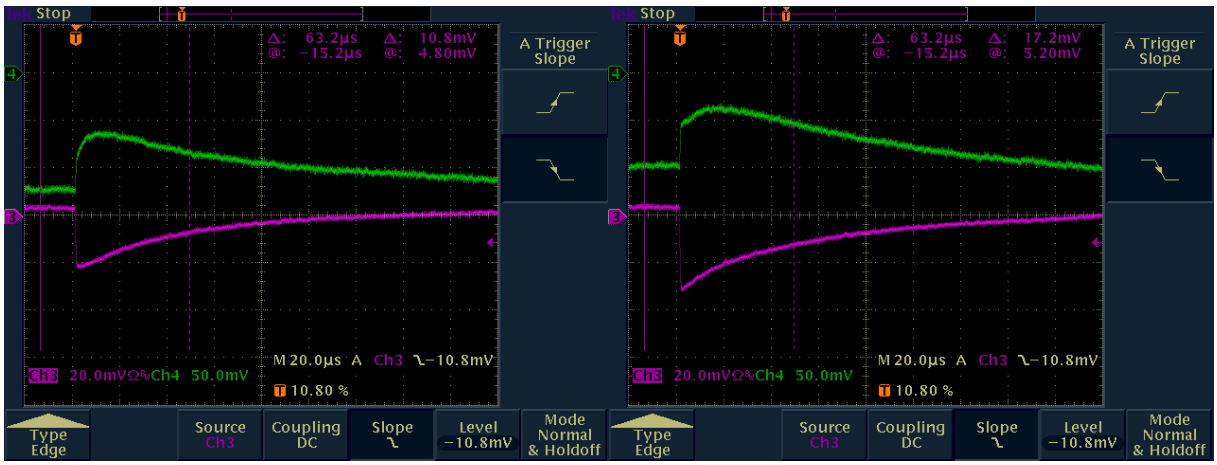

Figure 9: Typical pulses induced by a 6 keV photon on the mesh (ch. 3, magenta) and on the y strips (ch. 4, green) of the resistive micromega. The x strips are floating.

In the non-resistive micromega, sparks bring to ground the mesh voltage, resulting in monochromatic spikes of 470 V, followed by the recharging of the mesh with a characteristic time of 15 ms (1.5 nF gap capacitance times 10 MΩ protection resistor). The preamplifier gets paralyzed and stops working for about 1.4 seconds.

In the resistive micromega, the voltages spikes on the mesh are about 0.5 V. During the short time in which sparks develop and their ionization is collected, the resistive strips can be considered isolated. Sparks charge the pF capacitance between the resistive strip where the spark occurs and the corresponding readout strip, bringing locally the resistive-strip potential close to the mesh voltage. The resulting voltage spike on the mesh is reduced by a factor of a thousand, the ratio of the mesh capacitance (order of 1.5 nF) to the strip capacitance (order of 1.5 pF). Since sparks may involve more than one strip, the voltage spikes on the mesh are not monochromatic. Since voltage spikes are small, the preamp does not get paralyzed.

Figure 12 shows the current induced on the y electrode by a spark. In this case, the mesh voltage is stabilized with a 100 nF capacitor, and the y-electrode signal is sent through a 50 Ω cable to the Lecroy

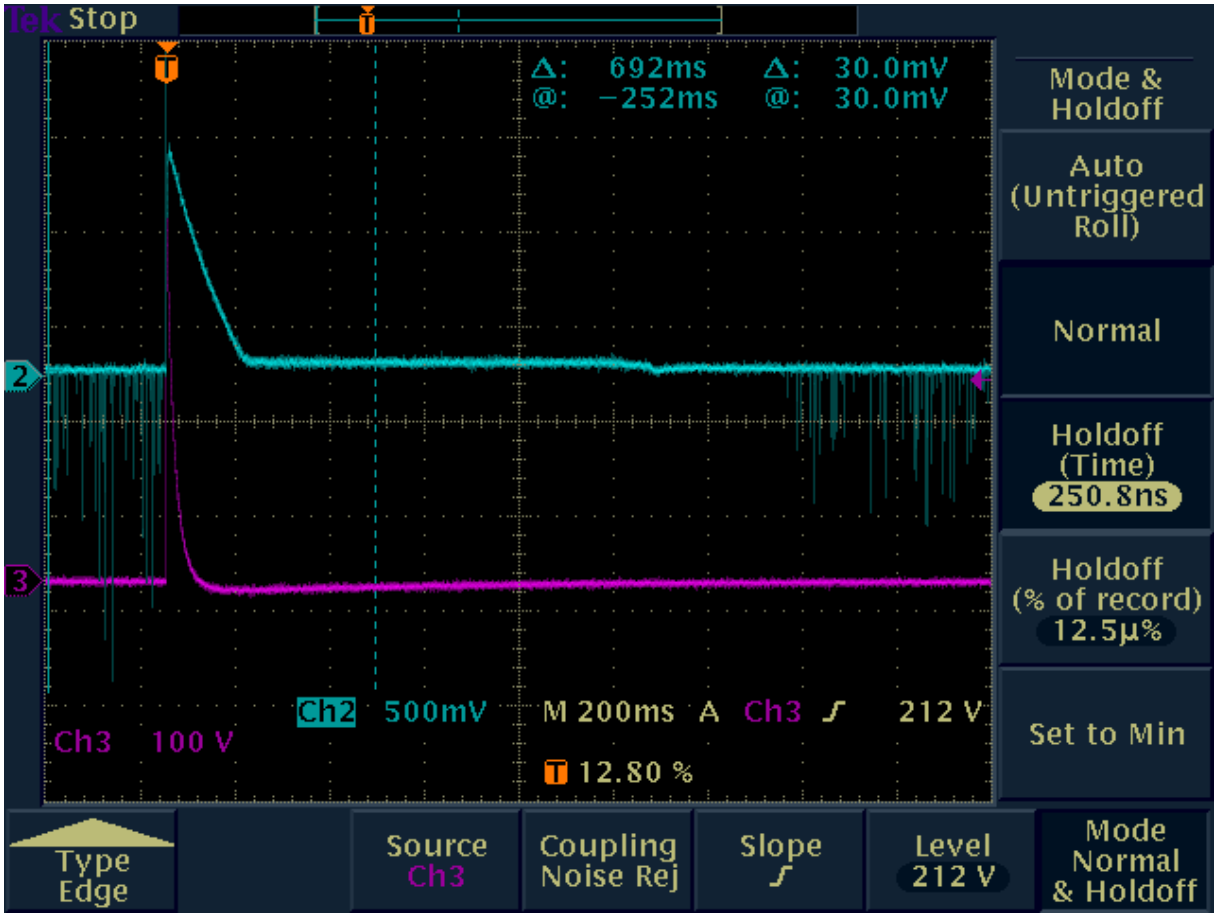

Figure 10: Typical spark signal observed with (ch. 2, blue) the preamp and (ch. 3, magenta) a probe, both connected to the non-resistive-micromega mesh. The short negative preamp pulses are due ^{55}Fe photons.

612AM preamplifier. No radioactive sources are used. The bulk of the current pulse induced by sparks on the y electrode lasts about 10 μs.

Further studies of dead time induced by sparks in the resistive micromega filled with a 93%A+7%CO_2 mixture are presented in the next section. This gas mixture has been proposed for the ATLAS upgrade.

7 Spark studies of the resistive micromega with a 93%Ar+7%CO_2 mixture

As mentioned earlier, during the spark development the resistive anode can be considered isolated. The current induced by a spark flows between the mesh and the y or x readout. At the same time, a spark charges the capacitances of the resistive strips and the mesh with respect to ground, generating a voltage step that ends when the charge on the resistive strips is dissipated or the mesh voltage restored. The charge injected by this voltage step into the preamp via the decoupling capacitors saturates its output which changes polarity when the voltage step ends. We use this feature to get a first estimate of the amount of time required to metabolize a spark. The 142C output saturates to 10 V with a voltage step of -4 mV (9.5 nF decoupling capacitor), whereas the 1406 saturates to -3 V with a voltage step of 18 mV

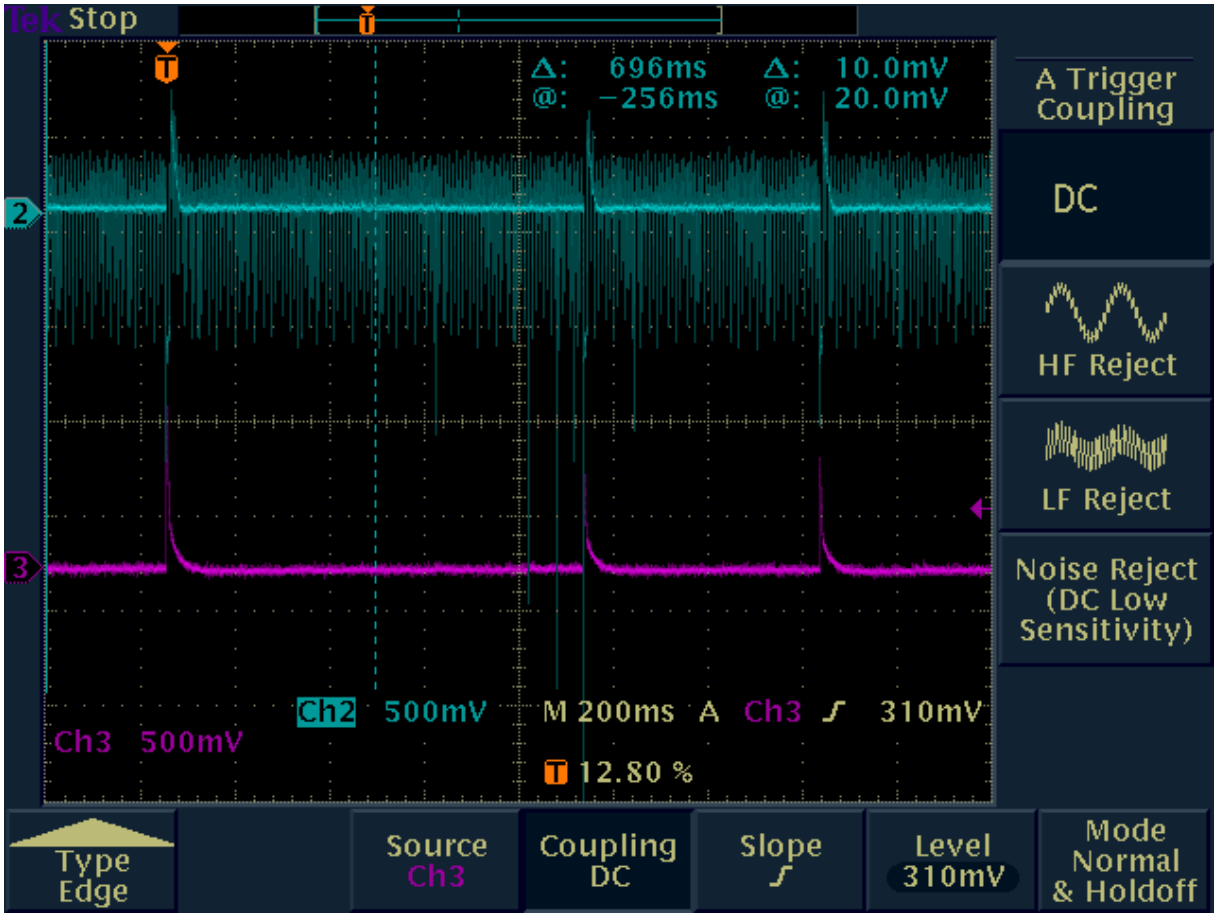

Figure 11: Typical spark signals observed with (ch. 2, blue) the preamp and (ch. 3, magenta) a probe, both connected to the resistive-micromega mesh. Preamp test pulses are also shown.

(2 nF decoupling capacitor). Because of the different decoupling capacitors, the preamps also drain out different fractions of the charge produced by a spark.

With the mesh voltage set at 570 V, the rate of spontaneous sparks is a few Hz. Figure 13 shows the signal of two different sparks as seen by the 1406 preamp on the mesh and the 142C on the x electrode. Both preamps invert the input polarity.

Figure 14 shows the signal of two different sparks as seen by the 1406 preamp on the mesh and the 142C on the y electrode. On the right picture, the horizontal scale is set to 2 ms/cm instead of 40 μs/cm. Since the two preamps have different saturations and fall-times, in Fig. 15 we show the signal of two different sparks as seen by the 142C preamp on the mesh and the 1406 on the y electrode. Again, the horizontal scale of the right picture is set to 2 ms/cm instead of 40 μs/cm.

One sees that the preamps on the mesh integrate a current tail as long as 10-12 ms due to the recharging of the mesh through the 10 MΩ protection resistor. This tail saturates only one of the two preamps. The voltage step due to the discharging of the resistive anode lasts between 100 and 200 μs as determined by the time at which the output of the preamps on the readout electrodes changes polarity.

By comparing with the previous figures, Figure 16 and 17 show that the 10 ms voltage step on the mesh disappears when stabilizing it with a 100 nF capacitor as shown in Fig. 6.

The current induced on the x electrode by the spark ionization and the subsequent voltage swing on the resistive anode is also investigated by connecting this electrode to the the Lecroy 612AM (gain of

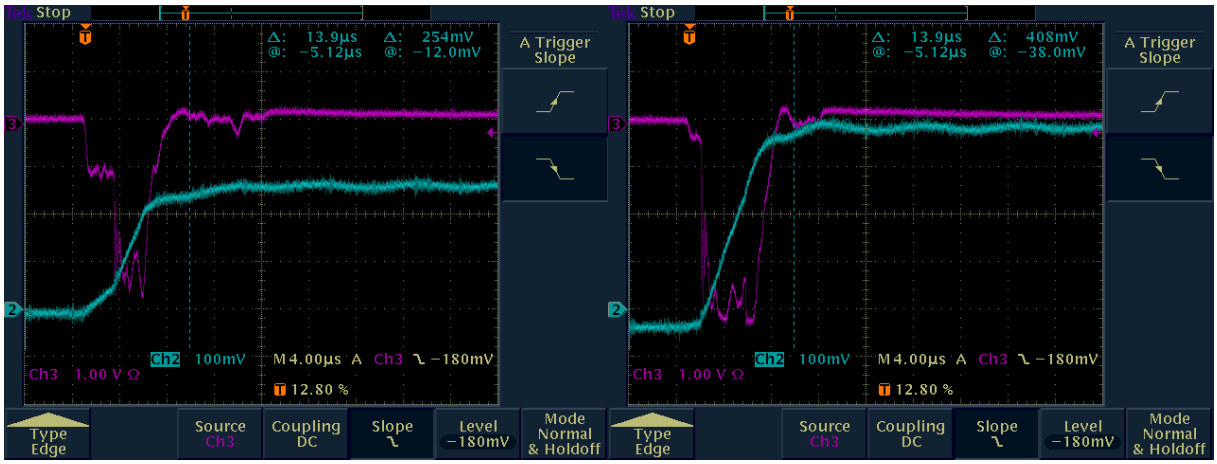

Figure 12: Typical spark signals observed on (ch. 3, magenta) the y-strips with a Lecroy 612AM and (ch. 2, blue) a probe connected to the micromega mesh. The 612AM gain is 50 and the mesh voltage is stabilized with a 100 nF capacitor.

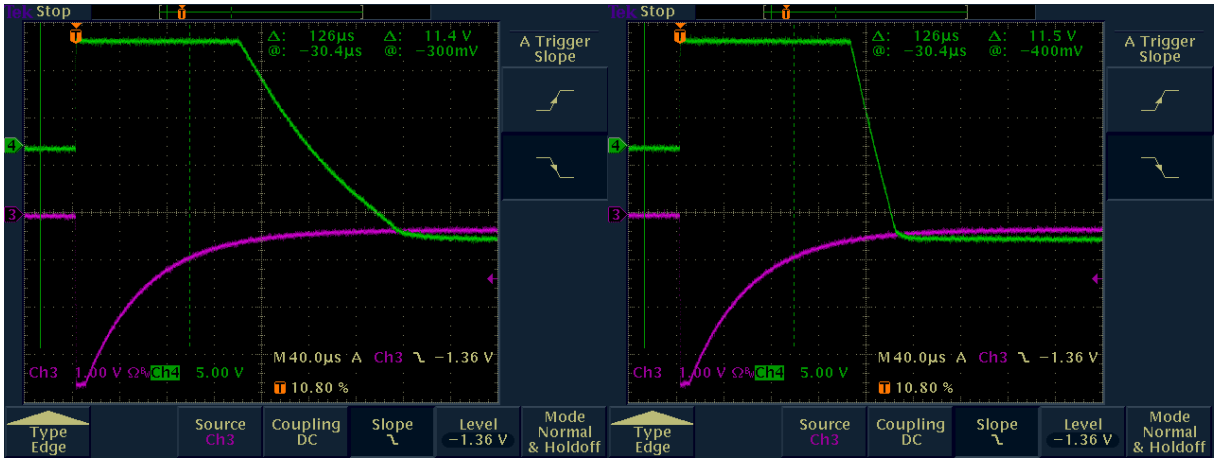

Figure 13: Pictures of two sparks as seen by (ch. 3, magenta) the 1406 on the mesh and 142C preamp on the x electrode.

50) with a 50 Ω cable. The signal, shown in Fig. 18, is a very fast pulse induced by the spark ionization followed by a pulse, several microsecond long, induced by the dispersion of the charge trapped on the resistive anode. This picture is taken with the y electrode floating. The average integrated area of a spark corresponds to 1.6 nC on the mesh or the y electrode [2]. We measure a spark charge consistent with what is reported in Section 4.3 of Ref. [2], however we observe average peak currents 50 times smaller and durations 50 times longer.

Figure 19 shows a typical ^{55}Fe signal seen on the x electrode with the 612AM amplifier. The 6 keV signal is of the order of 20 mV, and that of a MIP will be about 3.5 mV.

Figures 20 and 21 show spark signals seen by the 612AM with the same vertical scale as the ^{55}Fe signal and with a time scale of 20 and 100 μs, respectively. One sees that the pulse due to the charging and discharging of the resistive strips greatly exceeds a MIP pulse for several 100 μs.

[2] When using protection resistors smaller than 10 MΩ, the spark charge increases to about 2 nC.

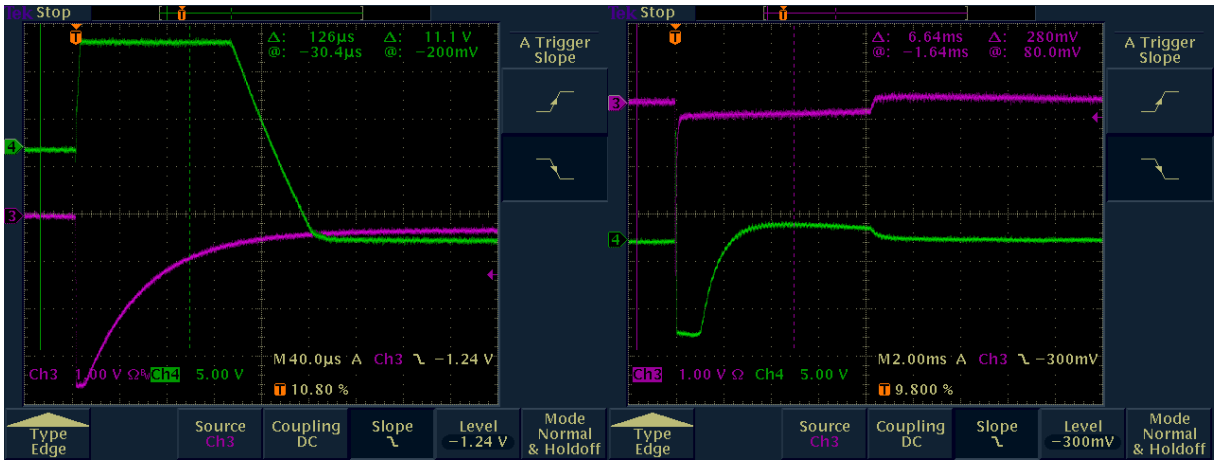

Figure 14: Pictures of two sparks as seen by (ch. 3, magenta) the 1406 on the mesh and (ch. 4, green) the 142C preamp on the y electrode using two different time scales.

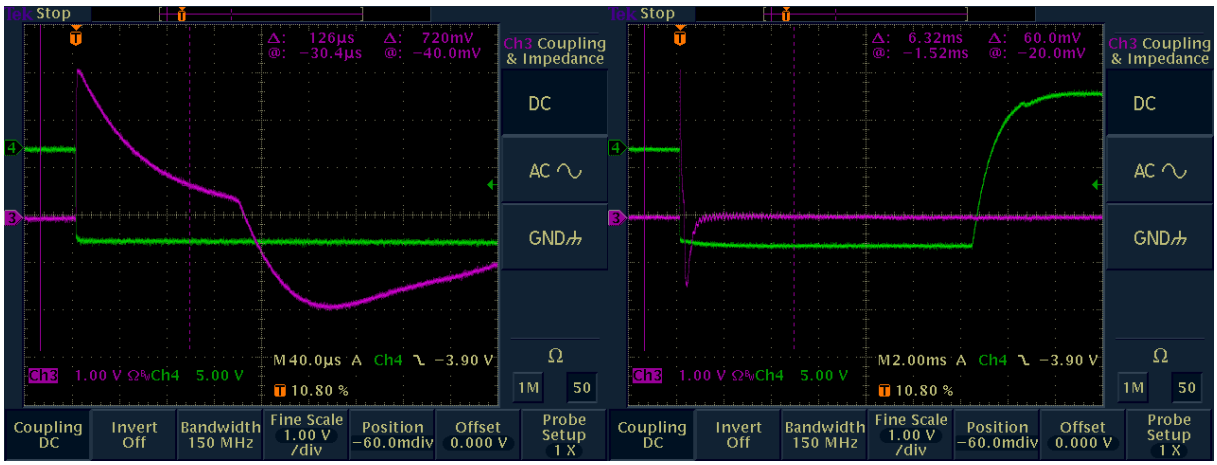

Figure 15: Pictures of two sparks as seen by (ch. 4, green) the 142C on the mesh and (ch. 3, magenta) 1406 preamp on the y electrode using to different time scales.

8 Spark rates for y-readout gain larger than 10^4

Using a 93%A+7%CO_2 mixture, our resistive micromega provides a y-readout gain of 10^4 for a mesh voltage of -560 V. No sparks are observed.

At a voltage of 570 V (gain of 1.5x10^4) we observe a rate of sparks of the order of several Hz without any irradiation. This rate increases to 400 Hz at 580 V and to 1.0 kHz at 590 V. At these voltages, we measure a mesh current of 0.6 and 1.4 μA, respectively, quite consistent with the estimate of 1.6 nC/spark.

The study in Ref. [2] has investigated the rate of sparks induced by highly-ionizing particles. In that study, a resistive micromega at 600 V filled with a 85%Ar+15%CO_2 mixture was irradiated with neutrons. The measured gain is quoted as 2x10^4 and the measured mesh current is about 200 nA. Using a charge of 1.6 nC/spark, this current corresponds to a 130 Hz rate of sparks, consistent, even if smaller, with our finding at 580 V without any irradiation. With a 93%A+7%CO_2 mixture and a gain of 1.2x10^4, that study measures a rate of sparks under neutron irradiation of several Hz which seems consistent with

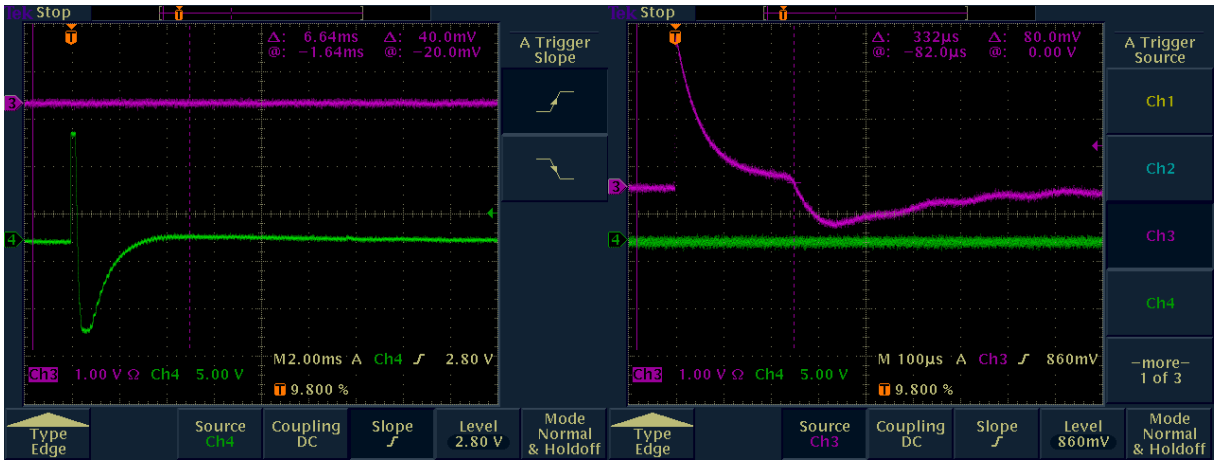

Figure 16: Pictures of two sparks as seen by the 142C preamp (left) and by the 1406 preamp (right) on the y electrode. The mesh voltage is stabilized with a 100 nF capacitor.

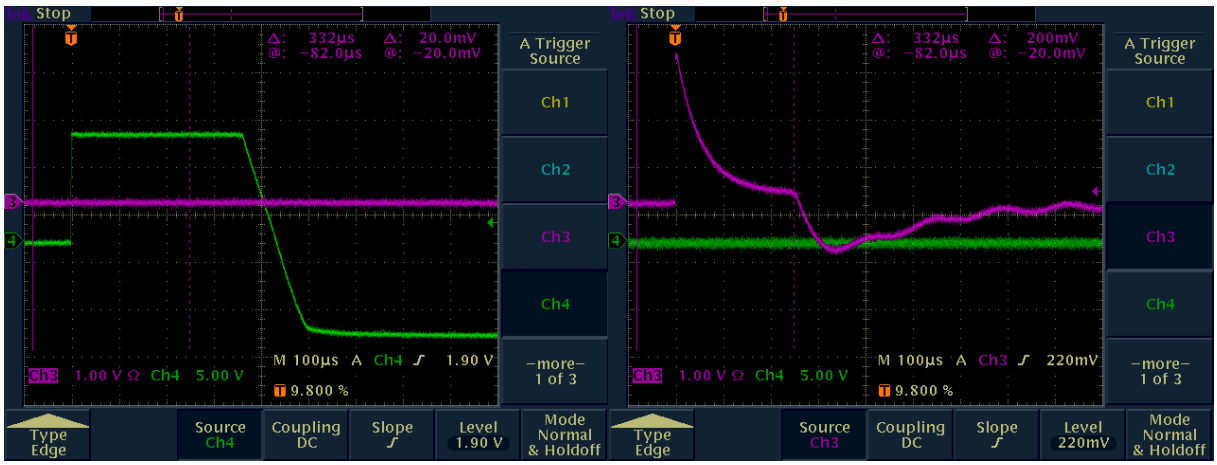

Figure 17: Pictures of two sparks as seen by (left) the 142C and (right) by the 1406 preamp on the x electrode. The mesh voltage is stabilized with a 100 nF capacitor.

our finding for a similar gain but without any irradiation. Therefore, at gains slightly larger than 10^4, the rate of neutron-induced sparks appears to be small compared to that of spontaneous sparks.

For spontaneous spark, the relevant parameter is not the gain but the effective voltage on the mesh. It seems intuitive that a micromega gap, when brought above its breakdown voltage, has to behave as a Zener diode, the dynamic impedance of which is provided by shedding sparks. Our 10 MΩ protection resistor limits the current (or the spark rate) needed to keep the mesh at the breakdown voltage. When using a 100 K protection resistor, as in the study in Ref. [2], one should have observed a significantly larger rate of sparks, but the mesh current was limited to 2 μA.

9 Breakdown voltage knee

We measure the current and spark rate of the resistive detector, filled with a 93%Ar+7%CO_2 mixture, as a function of the effective mesh voltage. The mesh is connected to the HV power supply with different resistors (10 MΩ, 1 MΩ, 220 KΩ, and 100 KΩ) and stabilized with a 100 nF capacitance. The mesh

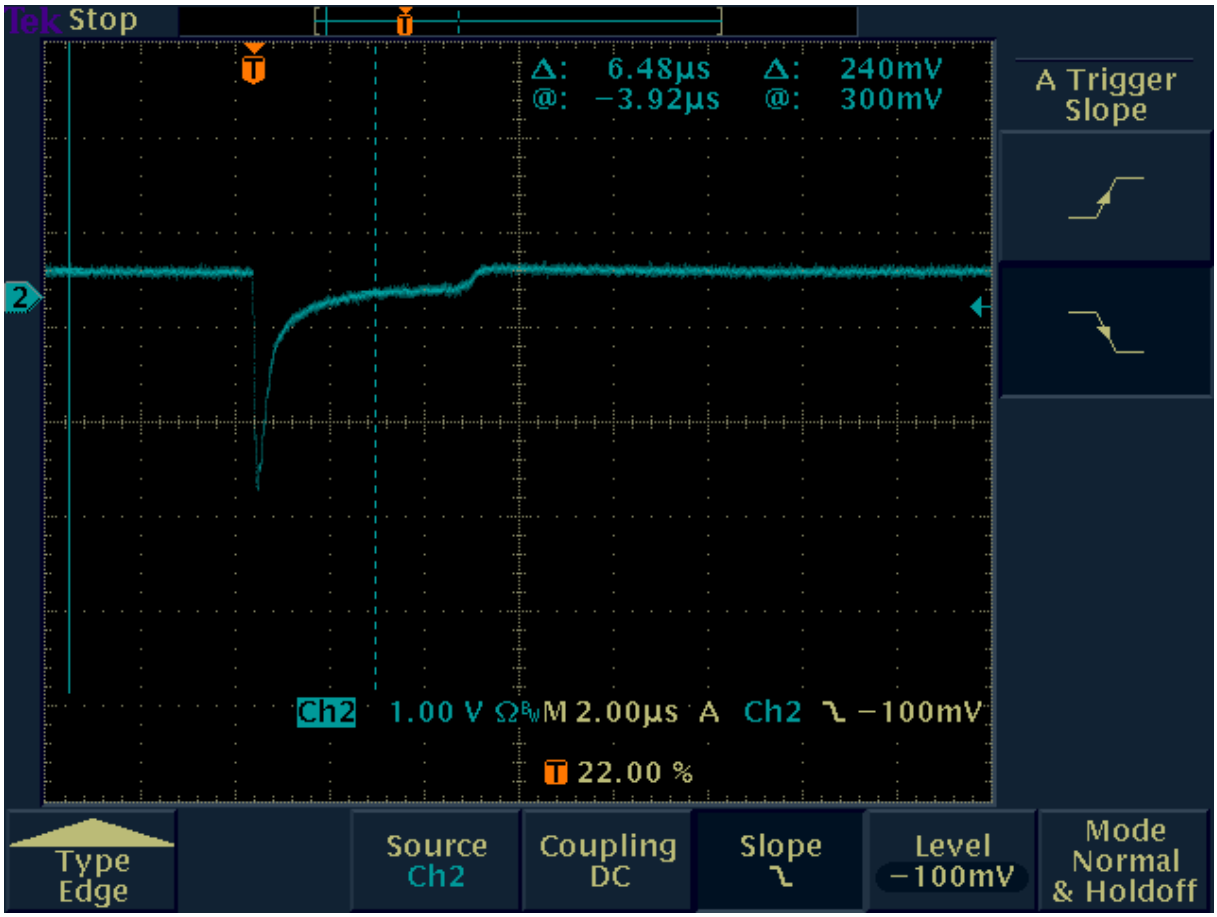

Figure 18: Typical spark signal seen with the Lecroy 612AM preamp on the x readout.

current is monitored by the HV power supply and we verify it by measuring the current flowing through the resistive anode. The spark rate is measured feeding the x-readout signals, amplified with the Lecroy 612AM, to an ORTEC 661 ratemeter. Spark currents and rates fluctuate significantly, and averages are evaluated by eye over a period of minutes. Including the tiring factor, their uncertainties are of the order of 20%. No sources are used and no drift field is applied to make sure we are dealing with spontaneous sparks.

Table 3 lists the result of these measurements. Figure 22 shows the mesh current as a function of the mesh effective voltage. Without current limitations, the spontaneous-spark rate is much larger than what reported in Ref. [2]. The resistive micromega does not draw any current below 570 V, and above 570 V its I-V curve is that typical of a Zener diode with a knee voltage of about 574 V. One advantageous consequence is that the spontaneous-spark rate does not depend on the mesh (or detector) area, but only on the applied voltage and protection resistor. The spontaneous-spark rate can be kept low since there is no point in applying voltages higher than the knee voltage. However, this raises a couple of concerns. In our prototype, the 14 V difference between the breakdown voltage and the 10^4 gain (a 50% gain change corresponds to 10 V) leaves very little room to adjust the gain. The other potential threat is the tolerance of the knee voltage on a larger size chamber. It seems plausible that sparks start at the weakest point of the weakest strip, drawing a fraction of a microamp [3]. As one tries to increase the mesh voltage beyond this critical value, sparking extends to the all detector which can draw up to 120 μA. Therefore, one spot

[3] A single resistive strip drawing a 10 μA current would sits at the mesh potential.

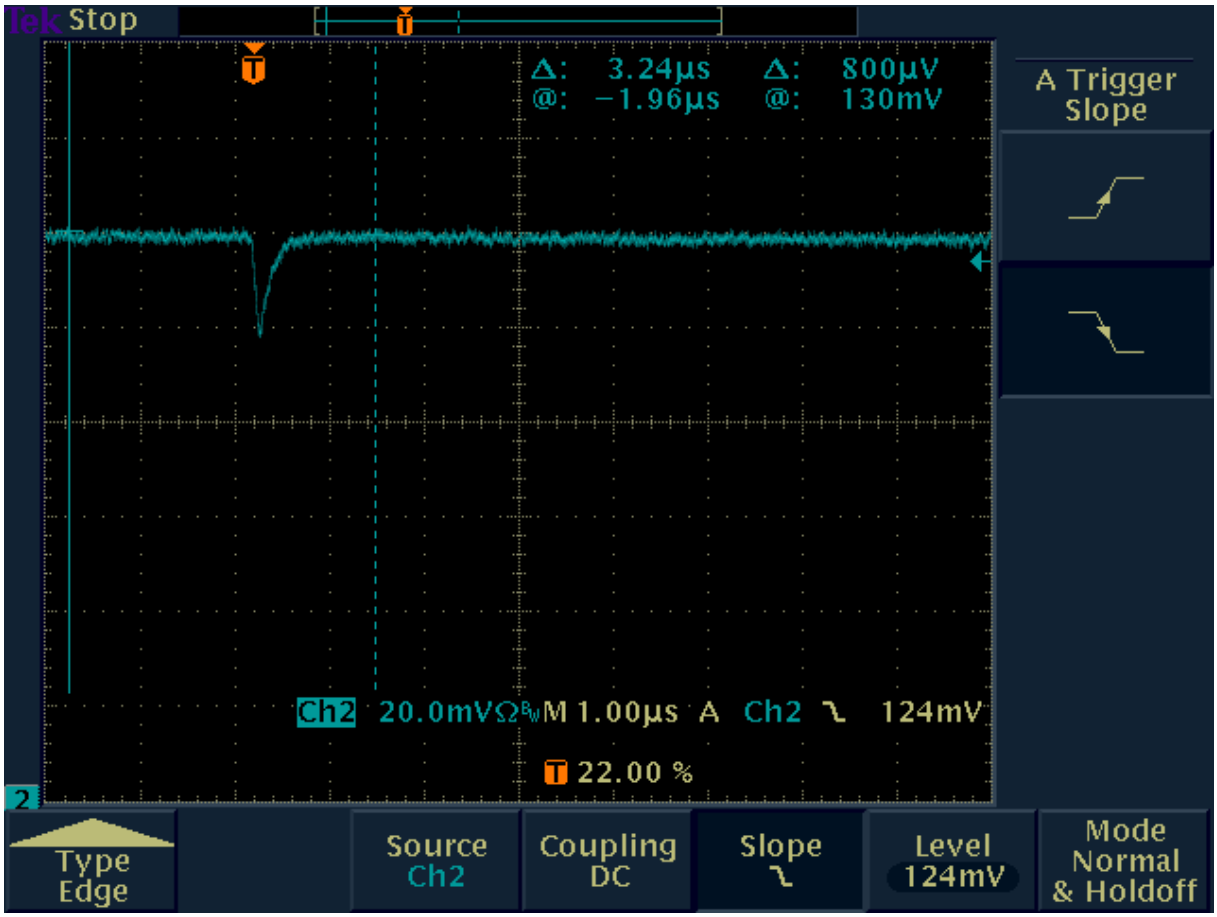

Figure 19: Typical ^{55}Fe signal as seen with a Lecroy 612AM on the *x* readout.

with a low breakdown voltage will prevent the entire chamber from reaching the desired gain.

References

[1] M. Byszewsky and J. Wotschack, doi:10.1088/1748-0221/7/02/C02060

[2] T. Alexopoulos *et al.,* NIM A640, pg.11 (2011).

[3] F. Paschen, *Ueber die zum Funkenuebergang in Luft, Wasserstoff, und Kohlensure bei verschiedenen Drucken erforderliche Potentialdifferenz*, Annalen der Physik **273**, pg. 69 (1889)

[4] S. Ramo, Proc. I.R.E. **27**, pg. 584 (1939).

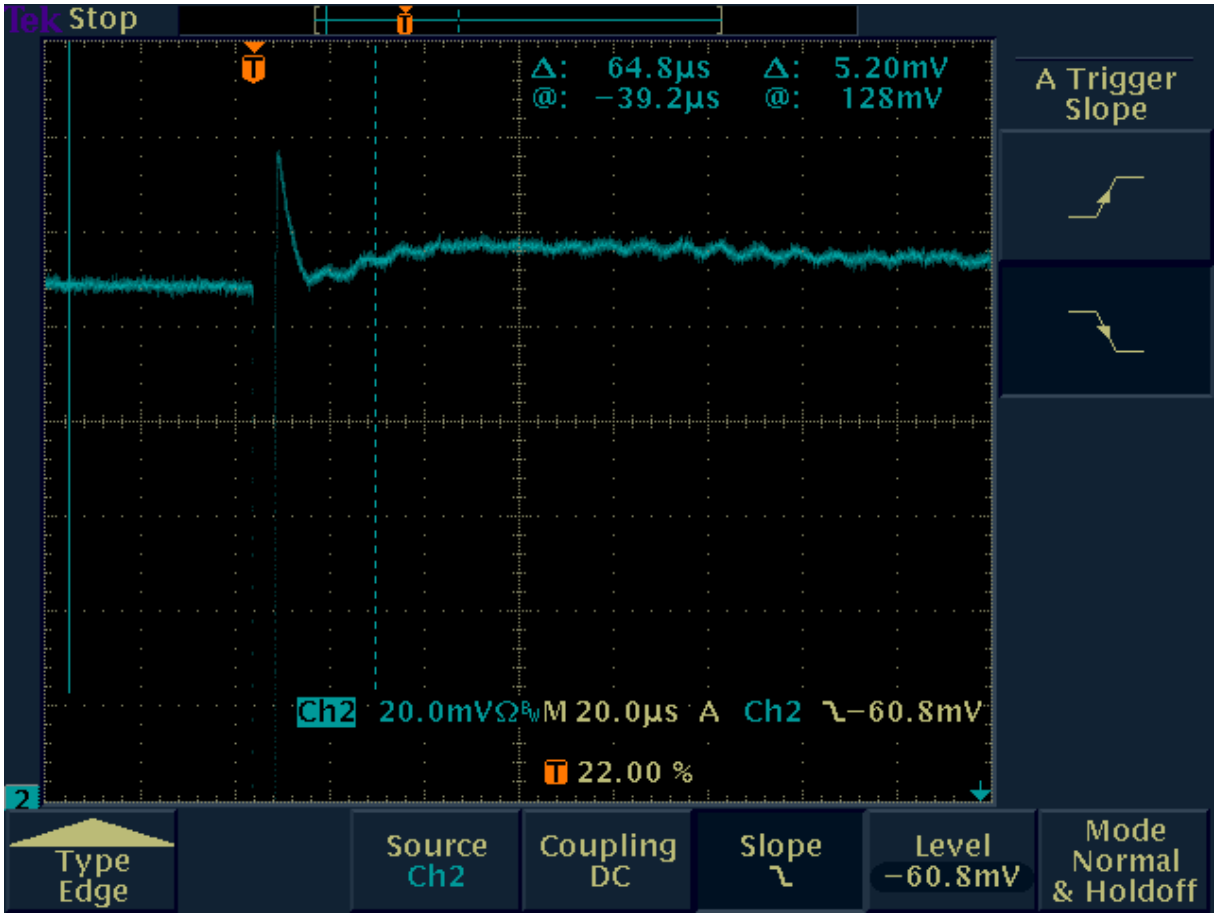

Figure 20: Spark signal as seen by a Lecroy 612AM on the x electrode. Most of the early spark signal is off scale. A MIP signal would be 3.5 mV.

Table 3: Average spontaneous-spark currents and rates as a function of V, the voltage supplied to the mesh through the resistor R and stabilized with a 100 nF capacitance. Rate and currents fluctuates in time and the averages, evaluated by eye, have at least a 20% uncertainty.

V (volts)	R= 10 MΩ		R=1.2 MΩ		R=0.22 MΩ		R=0.10 MΩ	
	μA	kHz	μA	kHz	μA	kHz	μA	kHz
570	0.0	0.1	0.0	0.2	0.2	0.3	0.5	0.5
575	0.1	0.2	1.2	0.9	2.6	1.0	5.0	2.0
580	0.6	0.4	3.6	1.5	11.0	6.0	16.0	10.0
585	0.8	0.6	6.5	3.5	22.0	9.0	42.0	20.0
590	1.4	1.0	10.0	5.0	36.0	15.0	66.0	30.0
595	1.6	1.0	13.7	7.0	49.0	20.0	98.0	50.0
600	2.2	1.1	18.0	10.0	68.0	30.0	120.0	60.0

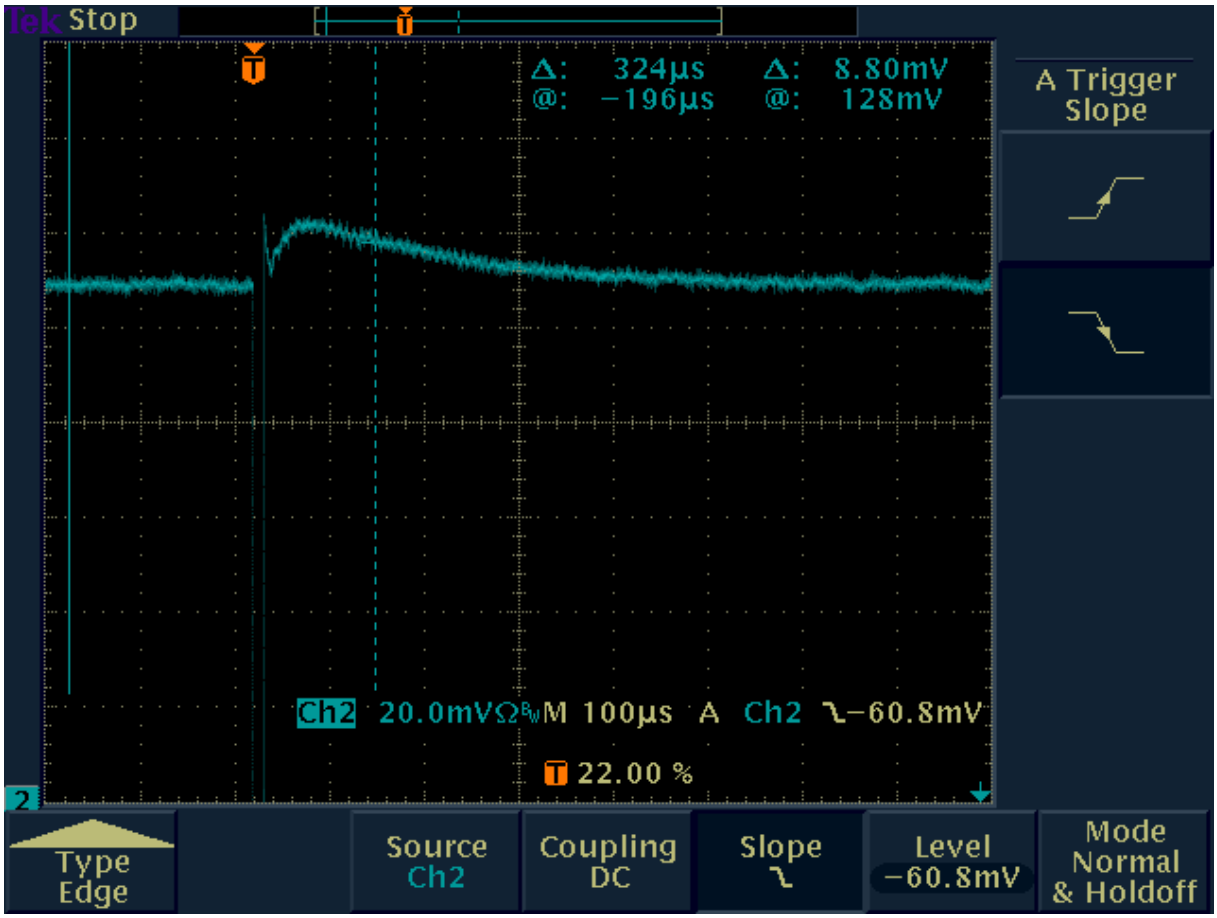

Figure 21: Spark signal as seen by a Lecroy 612AM on the x electrode. Most of the early spark signal is off scale. A MIP signal would be 3.5 mV.

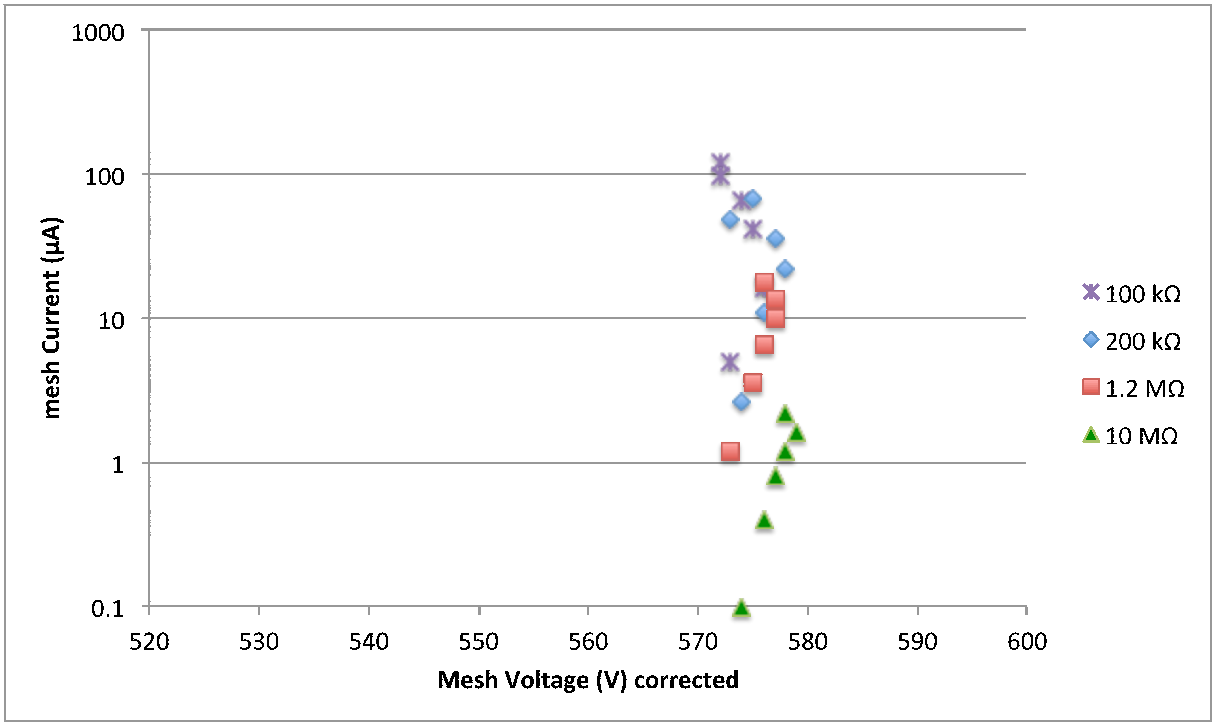

Figure 22: Mesh average currents induced by spontaneous sparks as a function of the effective mesh voltages for different values of the mesh protection resistor. The effective mesh voltage is calculated by subtracting from the voltages listed in Table 3 the drop caused by the detector current flowing through the resistors in series (R in Table 3 plus the $\simeq$ 140 KΩ resistor connecting the resitive anode to ground).